

# Analysis and Experimental Determination of Cable-Driven Stiffness

Duanling LI<sup>1</sup>, Lixing LIANG<sup>1</sup>, Kaijie DONG\*<sup>1</sup>, Hui QIU<sup>2</sup>

<sup>1</sup>School of Automation, Beijing University of Posts and Telecommunications, Beijing, China

<sup>2</sup>Beijing Institute of Spacecraft System Engineering, China Academy of Space Technology, Beijing, China

**Abstract.** The current reach of transmission mainly focuses on the gear drive. Compared with the typical gear transmission, cable drive has been widely used in many fields because of its advantages of large transmission torque, simple structure, smooth transmission, being easy to install and maintain. The accuracy of cable-driven stiffness calculation is increasingly required. Aiming at the problems of the calculation of equivalent stiffness lacked the analysis of preload mode and wrapped angle, a cable-driven preloaded device is designed in this paper. By analyzing the distribution of cable tension in different preload modes, the variation of slip region of tight side and slack side after loading is deduced. The equivalent stiffness equation of cable drive is obtained. The influence of design parameters on the stiffness of cable drive is analyzed. Experimental equipment was designed to measure parameters related to cable stiffness under different design parameters. The correctness of the theoretical analysis was verified experimentally. These results can provide reference for engineering design.

**Keywords:** cable drive, stiffness, preload, slip, deformation

## 1. Introduction

With the development of advanced design and manufacturing, the mechanical motion accuracy and dynamic performance are more and more demanding, which cause the need of simple and efficient mechanical transmission for realizing mechanism motion. Gear transmission is usually used in traditional mechanical transmission. However, even the most precise gear transmission has defects such as clearance and wear, which inevitably leads to cavitation, thus restricting the improvement of precision and dynamic performance. Cable drive mainly depends on the tension in cable and the friction between cable and wheel to transfer force and moment. There are many advantage of cable drive, such as high transmission accuracy of cable drive is high, low transmission backlash, and smooth transmission, which can well meet the requirements of the transmission of the mechanism. Cable drive has been widely applied in many fields, such as robot[1-4], deployment mechanism [5-8] and precise transmission[9-11]. In the application scenario of cable drive, the dynamics analysis is very important. The torque of the cable drive is usually replaced by the equivalent stiffness multiplied by the rotary angle of the wheel. The accuracy of equivalent stiffness directly affects the precision of dynamic calculation of transmission device. The cable are equivalent to a stretched spring by Jaime[12] who think that the equivalent stiffness is related to preload, load, the radius of wheel and other factors. However, the pretension force is not considered in the uneven distribution of the cable, and the preload is only regarded as a constant. The loading mode of preloading and the distribution of cable tension caused by preloading will affect the change of cable drive stiffness after loading. JIN et al. [13-15] studied the slip of the cable on the wheel and analyzed the deformation of the cable, which derived the calculation formula of the equivalent stiffness. In addition, the factor that the slip-angle cannot increase infinitely and is less than or equal to the wrapped angle is ignored, which will lead to calculation errors.

To solve the above problems, this paper designed a cable preloaded device, which has the advantages of simple structure, easy installation and debugging, and being not easy to occur the phenomenon of de-grooving. The transmission stiffness of cable is studied. The distribution of cable tension under different preloaded modes is analyzed. The cable-driven stiffness equation is deduced. The effect of slip-angle and wrapped angle on equivalent stiffness of cable is analyzed. The influence of preload, free region length, wheel radius and other factors on the transmission stiffness is verified by experiments, which provides a theoretical basis for the setting of preload and the calculation of cable equivalent stiffness. It has a certain reference value for the theoretical research and engineering design of cable drive in the future.

## 2. Design And Theory

### 2.1. Cable preloaded device

Cable drive is a way to transmit force and torque by the tension of cable and the friction between cable and wheel. The structure of a cable preloaded device is designed in this paper, as shown in Fig.1. The preloaded device is mainly composed of wheel, cable and preloaded device which is composed of knot, adjusting nut, cable screw and connector. One end of the cable is fixed on the preloaded device, the other end passes through the cable screw and the connector, and passes through the other wheel and the preloaded device in the shape of "8" pattern. The structure principle and dimension parameters are shown in Fig.2. The "8" shape pattern can increase the wrapped angle of the cable on the wheel and reduce the axial force of the cable. When capstan is affected by the torque, due to the friction between capstan and the cable, the tension difference will be generated at the end of the cable outlet and the end of the cable inlet, so that the torque will drive capstan to rotate. Both ends of the cable are fixed on capstan through the preloaded device, which is used to adjust and compensate the preload in the cable and play a fixed role. In the process of preloading, the cable is connected with spring tension gauge. After preloading along the knot screw axial direction by tension gauge, we should adjust the adjusting nut, make it contact with the knot, and slack the tension gauge to finish preloading. Repeating rotation of capstan can redistribute the preload force.

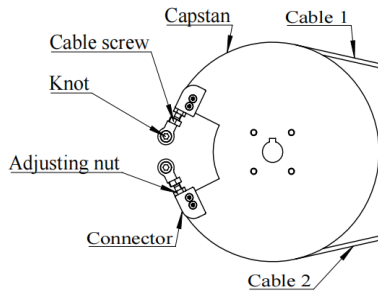


Fig.1 Preloaded device

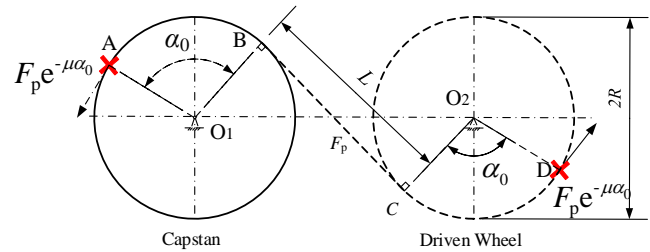


Fig.2 Cable preload mode

### 2.2. Cable slip

In the process of movement, the infinitesimal  $d\theta$  on the cable was used to analyze the force. The forces on both sides of  $d\theta$  with length  $Rd\theta$  are  $F$  and  $F + dF$  which are tangent to the surface of the driving wheel respectively.  $dN$  is the normal force from the cable in contact with the wheel and  $\mu dN$  is the traction force due to friction between the cable and the wheel. Force analysis is shown in Fig.3:

$$\sum F_x = (F + \mu dN) \cos \frac{\theta}{2} - (F + dF) \cos \frac{\theta}{2} = 0 \quad (1)$$

$$\sum F_y = dN - F \sin \frac{\theta}{2} - (F + dF) \sin \frac{\theta}{2} = 0$$

Since  $dF d\theta$  is infinitesimally small:

$$\frac{dF}{F} = \mu d\theta \quad (2)$$

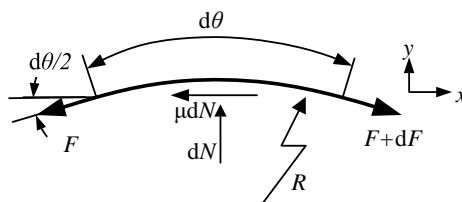


Fig.3 Differential cable element

## 3. Analysis Of Cable-driven Stiffness

Applying initial preload at the ends of the cable, the tension distribution on the cable is shown in Fig.4, where  $\alpha_0$  is the initial wrapped angle. The cable tension decreases gradually along the contact between the

cable and wheel, and remains unchanged in the free length. The changing trend can be obtained by integrating Eqs.(2) :

$$F(\alpha) = F_p e^{-\mu\alpha} \quad (3)$$

When capstan is rotated repeatedly, the preload is redistributed. The cable tension distribution is shown in Fig.5, where  $\theta$  is the slip-angle. In the case of capstan, the tension decreases from the free length, decreases in the BE section, and remains constant in the EA section.

When the load torque  $T$  is applied on capstan, it is equivalent to the increase of cable tension in the free length  $F_T$  ( $F_T=T/2R$ ). In traditional analysis of cable-driven stiffness, the wrap angle is divided into a slack elastic slip region, a tight side elastic slip region and a non-slip region. The deformation of the cable mainly occurs in the elastic slip region and free section. Fig.6 shows the tension distribution of tight side of cable drive. The solid line is the tension distribution after loading load, and the dotted line is the tension distribution after redistributing preload.

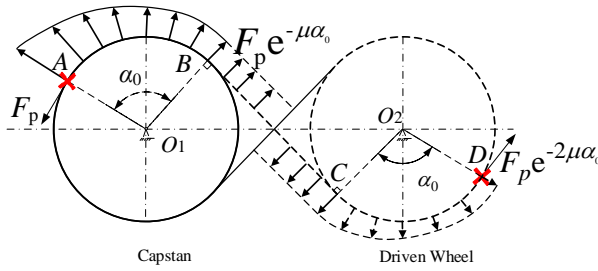


Fig.4 Tension distribution at initial state

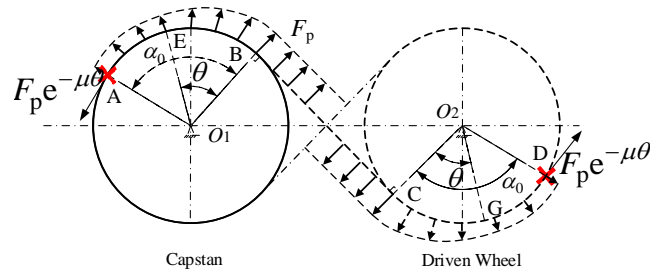


Fig.5 Tension distribution at work state

Integrating from  $F(\theta)$  to a tension  $F_T+F_p$  and 0 to  $\theta_s$ , where  $\theta_s$  is the slip-angle. The slip-angle is angle of the loaded cable on the wheel where slip can occur.

$$\int_{F(\theta)}^{F_p+F_T} \frac{dF}{F} = \int_0^{\theta_s} \mu d\theta \quad (4)$$

$$F(\theta) = (F_p + F_T)e^{-\mu\theta} \quad (5)$$

Eqs.(5) is the classic capstan equation used to find the two regions  $\theta_{s1}$  and  $\theta_{s2}$  where deformations in the cable occur as the cable transfers torque-induced loads to the wheel. When the slip-angle of the tight side  $\theta_{s1}$  is less than the wrapped angle  $\alpha_1$ , the slip-angle of the tight side  $\theta_{s1}$  can be obtained from Formula Eqs.(5):

$$\theta_{s1} = \frac{1}{\mu} \ln \frac{F_p + F_T}{F_p} \quad (6)$$

Firstly, taking the cable micro-element in the slip region of the tight side as an example, the change of length under the effect of tension  $F$  is established as

$$d\delta = \frac{FR}{EA} d\theta \quad (7)$$

The actual length change of cable micro-element ( $d\delta_F$ ) is the sum of length change caused by torque ( $d\delta_{F_T}$ ) and the length change caused by pre-load force ( $d\delta_{F_p}$ ). That is,

$$d\delta_F = d\delta_{F_T} + d\delta_{F_p} \quad (8)$$

Then the elongation of cable generated by torque on the tight side of the wheel is

$$\delta_{F_T} = \int_0^{\theta_{s1}} \frac{FR}{EA} d\theta - \frac{F_p R \theta_{s1}}{EA} \quad (9)$$

According to Eqs.(9), the length change  $\delta_1$  of the contact area  $\theta_{s1}$  between capstan and the tight side of the driven wheel are obtained:

$$\delta_1 = \delta_1' = \frac{R}{\mu EA} \left( F_T - F_p \ln \frac{F_T + F_p}{F_p} \right) \quad (10)$$

Stiffness is defined as:

$$K = \frac{dF}{d\delta} \quad (11)$$

Therefore, the stiffness in the slip region of the tight side is established as

$$K_1 = K_1' = \frac{\mu EA(F_p + F_T)}{RF_T} \quad (12)$$

When tight side slip-angle  $\theta_{s1}$  is equal to tight side wrapped angle  $\alpha_1$ , the tight side slip-angle is:

$$\theta_{s1} = \alpha_1 = \alpha_0 + \Delta\alpha \quad (13)$$

Hence

$$\delta_1 = \int_0^{\theta_{s1}} \frac{F_T e^{-\mu\theta} R}{EA} d\theta = \frac{F_T R(1 - e^{-\mu\alpha_1})}{\mu EA} \quad (14)$$

$$K_1 = K_1' = \frac{\mu EA}{R(1 - e^{-\mu\alpha_1})} \quad (15)$$

When the slip-angle in slack side  $\theta_{s2}$  is less than the wrapped angle in slack side  $\alpha_2$ , the tension distribution of slack side is shown in Fig.7

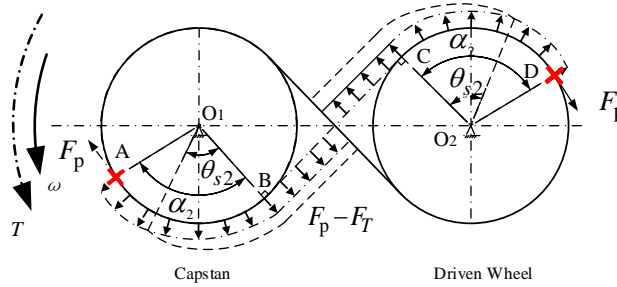


Fig.6 Tension distribution with loading in slack side.

According to the Fig.6:

$$(F_p - F_T)e^{\mu\theta_{s2}} = F_p \quad (16)$$

According to Eqs.(9), the change of cable length in the slip region at the slack side can be obtained:

$$\delta_2 = \delta_2' = \frac{R}{\mu EA} (F_T + F_p \ln \frac{F_p - F_T}{F_p}) \quad (17)$$

According to Eqs.(10), the stiffness of the slack side can be obtained as

$$K_2 = K_2' = \frac{\mu EA(F_p - F_T)}{RF_T} \quad (18)$$

When the slip-angle of slack side  $\theta_{s2}$  is equal to slack side wrapped angle  $\alpha_2$ , the slack side slip-angle is:

$$\theta_{s2} = \alpha_2 = \alpha_0 - \Delta\alpha \quad (19)$$

$$\delta_2 = \frac{F_T R(1 - e^{-\mu\alpha_2})}{\mu EA} \quad (20)$$

thus

$$K_2 = K_2' = \frac{\mu EA}{R(1 - e^{-\mu\alpha_2})} \quad (21)$$

The stiffness of the cable in free length region is expressed as

$$K_0 = \frac{EA}{L} \quad (22)$$

The linkage relationship of the stiffness is shown in Fig.7. The stiffness in the cable drive can be calculated as

$$K = K_{ti} + K_{sl} \quad (23)$$

Where,

$$K_{ti} = \frac{1}{1/K_1 + 1/K_0 + 1/K_1} \quad (24)$$

$$K_{sl} = \frac{1}{1/K_2 + 1/K_0 + 1/K_2'} \quad (25)$$

After loading the active torque, it can be obtained from the experimental data that the slip-angle  $\theta_{s1}$  increases faster than the wrapped angle  $\alpha$ , and the slip-angle  $\theta_{s2}$  increases and the wrapped angle  $\alpha$  decreases, so the slip-angle of the slack side  $\theta_{s1}$  equals to the corresponding wrapped angle earlier than the slip-angle of the tight side  $\theta_{s2}$ . In conclusion, the stiffness  $K$  of cable can be obtained as follows:

$$K = \begin{cases} \frac{\mu EA(F_p + F_T)}{2RF_T + \mu L(F_p + F_T)} + \frac{\mu EA(F_p - F_T)}{2RF_T + \mu L(F_p - F_T)} & \theta_{s1} < \alpha, \theta_{s2} < \alpha, F_T < F_p \\ \frac{\mu EA(F_p + F_T)}{2RF_T + \mu L(F_p + F_T)} + \frac{\mu EA}{2R(1 - e^{-\mu\alpha_2}) + \mu L} & \theta_{s1} < \alpha, \theta_{s2} > \alpha, F_T < F_p \\ \frac{\mu EA}{2R(1 - e^{-\mu\alpha_1}) + \mu L} + \frac{\mu EA}{2R(1 - e^{-\mu\alpha_2}) + \mu L} & \theta_{s1} > \alpha, \theta_{s2} > \alpha, F_T < F_p \\ \frac{\mu EA}{2R(1 - e^{-\mu\alpha_1}) + \mu L} & F_T > F_p \end{cases} \quad (26)$$

According to type of Eqs.(26), the main factor affecting torsional stiffness is the elastic modulus of cable (E), the cable equivalent cross-sectional area (A), cable and le wheel friction coefficient, cable wheel radius R, the cable length (L), wrapped angle ( $\alpha_0$ ), preload ( $F_p$ ) and load ( $F_T$ ). EA is directly proportional to K.

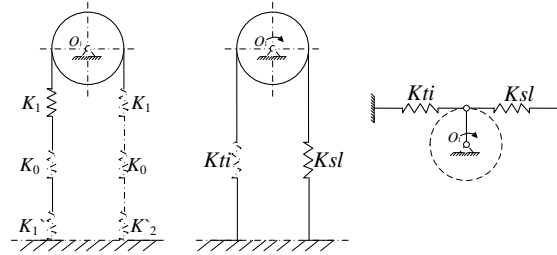


Fig.7 Simplification of stiffness model of cable drive

#### 4. Experimental Results And Analysis

Before the experiment, the performance parameters of the cable were measured. As the cable is made of multi-strand cable twisting, its equivalent sectional area is difficult to estimate. It is necessary to measure the tensile stiffness EA of the cable directly with the tension machine. As shown in Fig.9, test tools are installed at both ends of the cable, and the test process is shown in Fig.10.

The data are shown in Fig.10. Taking the data curve as linear growth, the equation  $EA = FL/\Delta L$  can be used to calculate that the cable EA is about 50000N.

The principle of the measuring device for friction coefficient between cable and wheel is shown in Fig.11. The cable wheel is fixed on the bracket with screws. One end of the cable is connected with a Z-type tension sensor, which is fixed on the platform; The other end of the cable is wrapped around the wheel at a certain angle and fixed to the cable screw. The preload  $F_p$  are added to the cable screw on the wheel. The wrapped angle  $\alpha$  can be obtained from geometric relations. The value of the tension sensor can be read as  $F_p + F_T$ . The friction coefficient  $\mu$  can be obtained from Eqs.(27). According to the experimental data,  $\mu \approx 0.25$ .

$$\mu = \frac{\ln((F_p + F_T)/F_p)}{\alpha} \quad (27)$$

The experimental device for cable drive is shown in Fig. 13. The wheel is connected with the axle through keys. The end of the driving axle is connected with the photoelectric encoder which can measure angle of rotation, and the other end is connected with the torque wrench. The rotary angle of capstan  $\Delta\alpha$  and load torque  $T$  are measured. The assembly method of the driven wheel and capstan is the same. The driven

wheel is fixed on the bracket with screws. By changing the distance between capstan bracket and the driven wheel bracket on the platform, the free length  $L$  of the cable can be adjusted.

The experimental process is mainly divided into nine steps: 1) Wrap cable in a figure-eight pattern once around capstan and driven wheel. 2) Tighten the cable to desired preload. 3) Rotate capstan back and forth 15–20 times. 4) Record initial reading of photoelectric encoder and torque wrench with no load. 5) Check desired load and record readings from photoelectric encoder and torque wrench. 6) Add weight to the torque arm in increments of 1kg until 10kg. 7) Record data from both photoelectric encoders for every 1 kg added and torque wrench. 8) Repeat two more times. 9) After third run, change different parameters and repeat the above steps.

In the process of increasing the load on capstan from 0 to 100N, the effects of preload, free length and wheel radius on the stiffness of cable were tested. The change of stiffness of cable is reflected in the rotary angle of capstan driven by the load force. The angle increases with the increase of load, whereas the increasing rate gradually decreases with the increase of stiffness. The theoretical curve of  $F_T-K$  was obtained by substituting the experimental data into Eqs.(26). The influence of related factors on equivalent stiffness  $K$  is analyzed by contrasting difference between the experimental data  $F_T-\Delta\alpha$  and the theoretical curve of  $F_T-K$ .



Fig. 8: Cable test sample



Fig.9: Tension/length of cable test

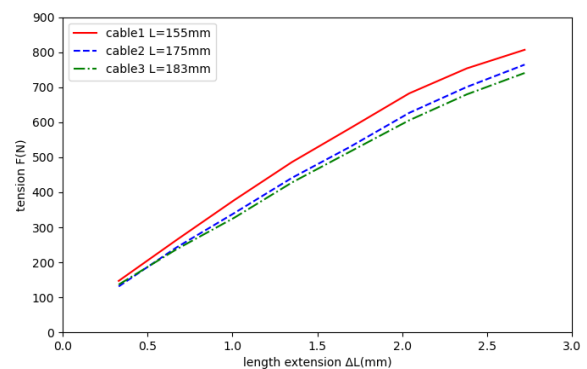


Fig.10 Applied tension vs. length extension

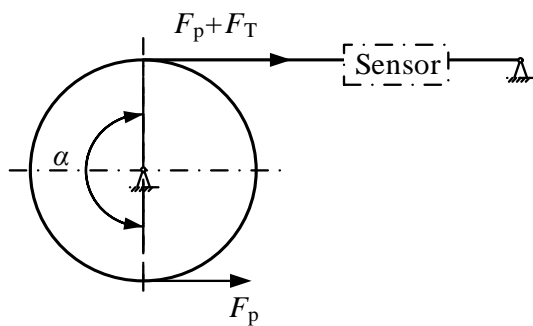


Fig.11 Friction coefficient test

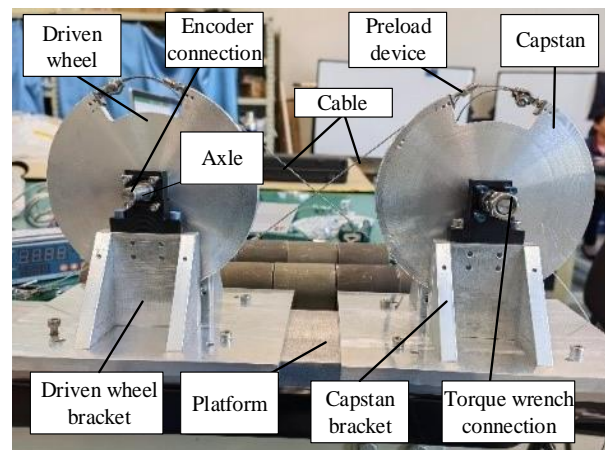


Fig.12 Tension distribution at work state

#### 4.1. Influence of preload on equivalent stiffness

The stiffness of cable loaded with different preloading forces varies with the loading force as shown in Fig.13. With the increase of load force, the stiffness decreases and tends to a constant value. When the load is larger than the preload, the slack side relaxes and the load will be completely borne by the tight side. The stiffness will suddenly decrease. The change of preload does not change the minimum equivalent stiffness. Increasing the preload can make the slip-angle equal to the wrapped angle later, which slows down the decreasing trend of the stiffness. It can be seen from Fig.13 that when the loading force is less than the preload, the angle rising trend gradually slows down. When the loading force is greater than the preload, the angle rising speed tends to a constant value. The experimental results are shown in Fig. 14. The increase of

preload  $F_p$  will reduce the wheel rotary angle under the same load, which means that increasing the preload  $F_p$  will increase the stiffness  $K$ .

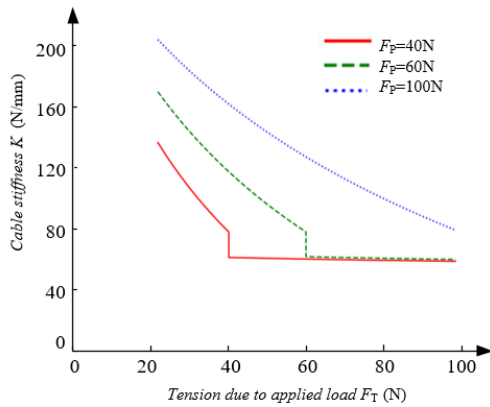


Fig. 13. Stiffness  $K$  to load  $F_T$  and preload  $F_p$ ,  $\mu=0.25, EA=50000N, R=75mm, L=360mm, \alpha_0=64^\circ$ .

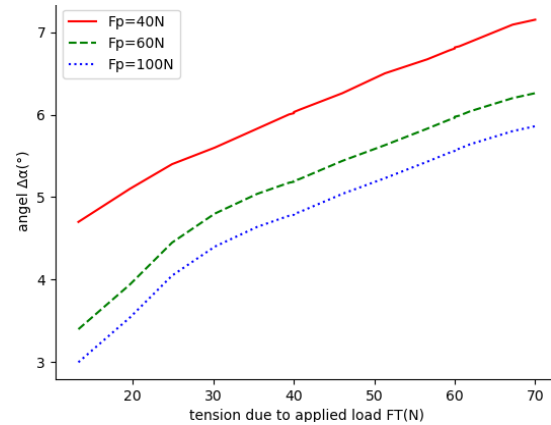


Fig. 14. Angle  $\Delta\alpha$  to load  $F_T$  and preload  $F_p$ .

#### 4.2. Influence of Free Region Length on Stiffness

For different free length  $L$ , the curve of stiffness changing with load is shown in 错误!未找到引用源。 . It can be seen from 错误!未找到引用源。 that under the same load, the stiffness  $K$  decreases with the increase of free length  $L$ . The minimum equivalent stiffness of cable decreases with the increase of  $L$ . According to the formula and experimental results, there are two factors that affect the stiffness by changing the free length  $L$ . The increase of  $L$  will reduce the stiffness of the free region, thus reducing the stiffness  $K$ . In addition, the increase of  $L$  will reduce the wrapped angle of the cable  $\alpha$ , and the slip-angle is equal to the wrapped angle  $\alpha$  after the loading force is smaller. The stiffness decreases with the increase of the loading force. Therefore, with a certain preload, reducing the length of the free region can effectively increase the wrapped angle and the stiffness of the free region, thus achieving the purpose of increasing the equivalent torque. As shown in Fig. 15, when the load increases, the rate of angle increase and stiffness decrease simultaneously. When the stiffness is constant, the rate of angle increase is approximately constant. The experimental results are shown in Fig. 15. The increase of free length will reduce the wheel rotary angle under the same load, which means that increasing the free length  $L$  will increase the stiffness  $K$ .

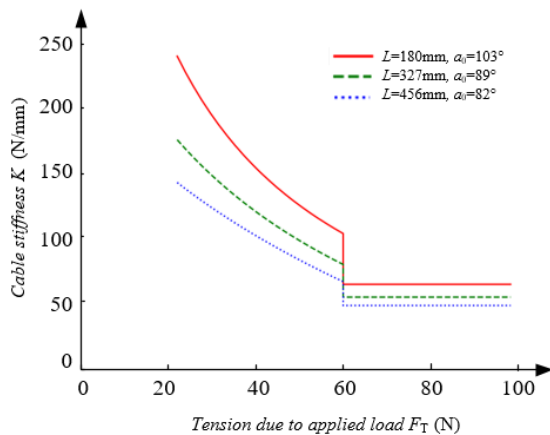


Fig. 16. Stiffness  $K$  to load  $F_T$  and free length  $L$ ,  $\mu=0.25, EA=50000N, F_p=60N$ .

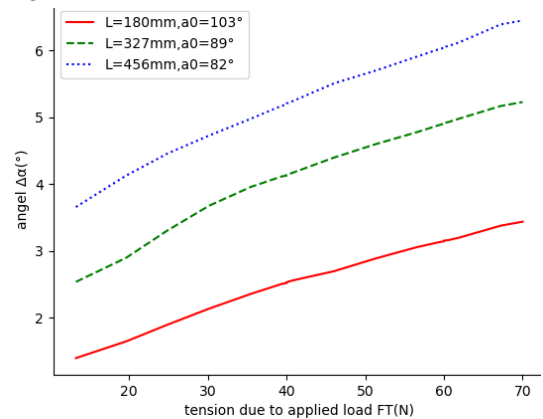


Fig. 15. Angle  $\Delta\alpha$  to load  $F_T$  and free length  $L$ .

#### 4.3. Influence of Wheel Radius on Stiffness

For different radius of wheel, the curve of stiffness of cable changing with load is shown in Fig. 18. With the same loading force, the smaller the radius of cable wheel, the larger stiffness of cable and the larger the minimum equivalent stiffness. With the same conditions, reducing the radius of wheel can increase the equivalent stiffness. The experimental results are shown in Fig.19. The increase of wheel radius will reduce the wheel rotary angle, which means that increasing the radius  $R$  of wheel will increase the stiffness  $K$ .

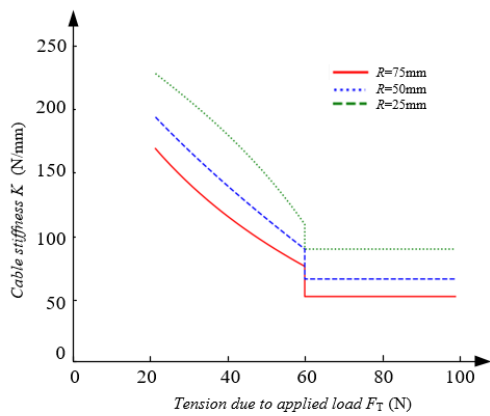


Fig. 16. Stiffness  $K$  to load  $F_T$  and radius  $R$ ,  $\mu=0.25$ ,  $EA=50000N$ ,  $L=360mm$

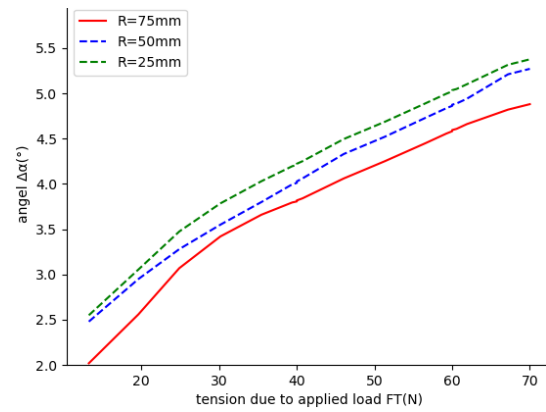


Fig.17. Angle  $\Delta\alpha$  to load  $F_T$  and radius  $R$ .

The stiffness  $K$  is mainly composed of stiffness of tight side, stiffness of free region and stiffness of slack side. The slip-angle of tight side increases with the increase of load moment, and the equivalent stiffness decreases continuously at this stage, while the descending speed decreases gradually. When the slip-angle is equal to the wrapped angle, the slip-angle does not change. Compared with the slip-angle of tight side, the slip-angle of slack side will equal to the wrapped angle early. When the load is bigger than the preload, the equivalent stiffness is the minimum value. Therefore, the stiffness can be effectively increased by making the slip-angle equal to the wrapped angle later. The main factors affecting torsional stiffness are elastic modulus of cable  $E$ , equivalent cross-sectional area of cable  $A$ , friction coefficient  $\mu$ , wheel radius  $R$ , the free section length of cable  $L$ , wrapped angle  $\alpha$ , slip-angle  $\theta$ , preload  $F_p$  and load  $F_T$ .  $EA$  are directly proportional to the stiffness  $K$ .  $K$  is negatively correlated with  $L$  and  $R$ , and positively correlated with  $F_p$ .  $K$  can be effectively increased by appropriately increasing  $F_p$  and decreasing  $L$  and  $R$ .

## 5. Conclusion

(1) This paper designs a kind of the preloaded device, which is beneficial to installation and maintenance, and improves the efficiency of cable drive. Based on this device, the distribution of cable tension and equivalent stiffness of cable drive are studied. The stiffness equation of cable drive considering the relationship between slip-angle and wrapped angle is derived.

(2) The influence of preload, free length and radius of wheel on transmission stiffness was analyzed. Increasing preload, decreasing free section length and reducing wheel radius can effectively increase cable-driven stiffness. These factors can be considered in the design of cable drive.

(3) The correctness of theoretical analysis is proved by measuring the relationship between the load and the wheel rotary angle.

## 6. References

- [1] Fang Xu. Innovation design of the cable-driven manipulator. Shandong: Ocean University of China, 2014.
- [2] Sun hanning, Hou yu, Mechanism Design and Mechanical Analysis of Multi-mode Grab Underactuated Hand, Journal of Mechanical Transmission, 2021: 90-96.
- [3] Chen Weihai, Dynamics modeling and tension analysis for a cable-driven humanoid-arm robot, Journal of Beijing University of Aeronautics and Astronautics, 2013, 39(3): 335-339.
- [4] Yang Guilin, Lin Wei, Kurbanhusen M S, et al. Kinematic design of a 7-DOF cable-driven humanoid arm: a solution-in nature approach, Proceedings of the International Conference on Advanced Intelligent Mechatronics, California, USA, 2005, pp.444-449.
- [5] Chen Lieming, Analysis of tension variation of solar wing linkage rope, Spacecraft Engineering, 1992, 8(4): 9-13.
- [6] Li Weituo, Design and analysis of preset tension of solar wing linkage, Chinese space science and technology, 2006, 2: 52-57.
- [7] Li Duanling, Dong Kaijie, Wang Xingze, Li Biao, Su Zhou. Design and Analysis of Synchronous Joint for SAR Antenna Deployable Mechanism, Proceedings of ASME 2019 International Design Engineering Technical

Conferences & Computers and Information in Engineering Conference, Anaheim, USA, August 18-21, 2019.

- [8] Liu Ruiwei, Guo Hongwei, Liu Rongqiang, etc. Shape accuracy optimization for cable-rib tension deployable antenna structure with tensioned cables. *Acta Astronaut.* 2017, 140: 66 - 77.
- [9] Zhang Hongwen, Cao Guohua, etc, Application of wire rope gearing in aerial optical remote sensor, laser and infrared, 2013, 43(4): 418-422.
- [10] Zhang Lianchao, Lu Yafei, Fan Da-peng, Hei Mo. Verification and Analysis of Cable Drive Transmission's Backlash Characteristics, *Aero Weapony*, 2014, 1: 14-19.
- [11] Lu Yafei, Study on the Principle and Design Method of the Precise Cable Drive. Changsha: National University of Defense Technology, 2013.
- [12] Werkmeister J, Slocum A, Theoretical and experimental determination of capstan drive stiffness. *Precision Engineering*, 2007, 31:55-67.
- [13] Jin Zhongqing. Study and test on precise steel cable driver, Changsha: National University of Defense Technology, 2006.
- [14] Xie hongwei, Experimental research on Transmission Accuracy of Multi-cable Drive, *Acta Armamentarii*, 2017, 38(4):728-734.
- [15] Dong Kaijie, Li Duanling, Lin Qihong, Qiu Hui, Cong Qiang, Li Xiao. Design and analysis of a novel hinged boom based on cable drive, *Chinese Journal of Aeronautics*, 2022, 35(3) : 592-606.